Accepted Manuscript

Paleomagnetism of the Yuanmou Basin near the southeastern margin of the Tibetan Plateau and its constraints on late Neogene sedimentation and tectonic rotation

R.X. Zhu, R. Potts, Y.X. Pan, L.Q. Lü, H.T. Yao, C.L. Deng, H.F. Qin

PII: S0012-821X(08)00267-7
DOI: doi: 10.1016/j.epsl.2008.04.016
Reference: EPSL 9279

To appear in: *Earth and Planetary Science Letters*

Received date: 12 November 2007
Revised date: 13 April 2008
Accepted date: 16 April 2008

Paleomagnetism of the Yuanmou Basin near the southeastern margin of the Tibetan Plateau and its constraints on late Neogene sedimentation and tectonic rotation

R. X. Zhu[a,*], R. Potts[b], Y. X. Pan[a], L. Q. Lü[a], H. T. Yao[a], C. L. Deng[a], H. F. Qin[a]

[a] *Paleomagnetism and Geochronology Laboratory (SKL-LE), Institute of Geology and Geophysics, Chinese Academy of Sciences, Beijing 100029, China*

[b] *Human Origins Program, National Museum of Natural History, Smithsonian Institution, Washington, DC 20013-7012, USA*

* Corresponding author. Tel.: +86 10 8299 8201; fax: +86 10 6237 2053.

E-mail address: rxzhu@mail.iggcas.ac.cn (R.X. Zhu)

Abstract

New paleomagnetic investigation was carried out on the late Neogene fluviolacustrine sequence of the Yuanmou Basin, located near the southeastern margin of the Tibetan Plateau. Magnetostratigraphic results indicate nine reverse magnetozones (R1 to R9) and eight normal magnetozones (N1 to N8) in the sedimentary profile, which can be correlated to the geomagnetic polarity timescale from C3n.3r to C1r.1r. The age of the sedimentary sequence of the Yuanmou Basin can thus be paleomagnetically constrained to an interval from early Pliocene to Pleistocene, with sedimentation rates varying from 12.5 to 55 cm/kyr. In addition to its highly resolved magnetostratigraphic sequence, the Yuanmou Basin provides a record of Plio-Pleistocene tectono- and climato-sedimentary processes. The mean declinations of the seventeen polarity units (excluding samples with transitional directions) can be grouped into three distinct directional intervals, Group I (2.58−1.37 Ma), Group II (4.29–2.58 Ma) and Group III (4.91–4.29 Ma). These directions indicate that the Yuanmou Basin has probably experienced vertical-axis clockwise rotation of about 12° from 1.4 Ma to 4.9 Ma, which may be related to slip activity of the Red River fault to the southwest and the Xianshuihe-Xiaojiang fault to the east.

Keywords: Yuanmou Basin; magnetostratigraphy; vertical-axis rotation; late Neogene

1. Introduction

The knowledge of the Cenozoic tectonic evolution of the Tibetan Plateau and its adjacent area is important to understand the physical properties of the lithosphere during the process of continent-continent collisions (see reviews by Yin and Harrison, 2000; Tapponnier et al., 2001) (Fig. 1). A poorly understood question about the Himalayan-Tibetan orogeny is whether the penetration of India into Asia is accommodated through distributed crust thickening or localized deformation at major lithospheric faults with high slip rates and that bound quasi-rigid blocks (England and Houseman, 1988; Peltzer and Tapponnier, 1988; Avouac and Tapponnier, 1993; Chen et al., 2002; Dupont-Nivet et al., 2002, 2003, 2004; Huang et al., 2004). Moreover, the phased uplifts of the Tibetan Plateau have had significant impact on late Cenozoic climatic change in East Asia (e.g., Chung et al., 1998; Rea et al., 1998; An et al., 1999, 2001; Guo et al., 2002; Clark et al., 2005).

The eastern margin of the Tibetan Plateau is one of its most active tectonic region with features of Tertiary Indochina extrusion to southeast and clockwise rotations around the eastern Himalayan syntaxis (England and Molnar, 1990; Leloup et al., 1995; Wang et al., 1998; Wang and Burchfiel, 2000; Tapponnier et al., 2001). Earlier paleomagnetic studies revealed clockwise rotation of the Qiangtang terrane (e.g., Zhu et al., 1988; Otofuji et al., 1990; Huang et al., 1992) and the Simao Terrane (Sato et al., 2007). Some counterclockwise rotations of the Cretaceous and Tertiary rocks from southeast China, possibly linked to motion related to the Red River fault was also reported by workers (e.g., Gilder et al., 1993). However, paleomagnetic constraints on the deformation ages and rotations in this region are still sparse, and, therefore, more data are needed.

The Yuanmou Basin in northern Yunnan Province, located in the east of the eastern Himalayan syntaxis (Fig. 1), preserves late Cenozoic fluviolacustrine deposits with a thickness of ≥850 m. In an attempt to determine age of the two hominin incisors found in the upper section of this basin in 1965 (Hu, 1973; Qian et al., 1984), which were attributed to *Homo* [*Sinanthropus*] *erectus yuanmouensis* (Hu, 1973; Wu and Poirier, 1995), magnetostratigraphic studies were carried out by Li et al. (1976) and Hyodo et al. (2002). However, in Li et al.'s study, only 76 samples in total were collected and were not analyzed by stepwise thermal demagnetization, which is now standard practice in evaluating sediments that contain hematite as a principal remanence carrier. Their paleomagnetic results suggested an age of ~1.7 Ma for the hominin incisors. In the work of Hyodo et al. (2002), paleomagnetic sampling intervals were too sparse and unevenly distributed with depth. Four to five samples were collected at each of 78 sites. Moreover, in their studies, the majority of samples were demagnetized by alternating field (AF) demagnetization technique and thermal treatments were done only at sites where a normal polarity magnetization was obtained by AF demagnetization. They identified four normal and four reverse polarity chrons based on 183 samples from 75 sites (including 29 sites with large α_{95} values between 15° and 37.6°), by which they revised the age of the hominin incisors to the early Brunhes chron (~0.7 Ma), 1 myr younger than the age reported by Li et al. (1976), and obtained an age of ~3.6 Ma (Gilbert-Gauss geomagnetic reversal) for the bottom of the Shagou Formation.

Here we present new paleomagnetic results from the Yuanmou Basin with aims to (1) establish high-resolution magnetostratigraphy for the entire Yuanmou fluviolacustrine sequence; and (2) examine the tectonic rotation history of the basin back to late Neogene time.

2. Geological setting and sampling

The Yuanmou Basin is geologically located in the northern Yunnan terrane bounded by two major fault zones, on the southwest by the NW-SE trending Red River fault zone and on the northeast by the curved Xianshuihe-Xiaojiang fault zone (Fig. 1). The Red River fault zone, which extends over a length of >1,000 km, has been regarded as the suture zone between the South China block and Indochina block (Zhang et al., 1983). The curved Xianshuihe-Xiaojiang fault is nearly NS-trending in northern Yunnan with a width of about 150 km. Eastwardly, it consists of the Yuanmou fault, Yimen fault, Pudu River fault, West Xiaojiang fault, and East Xiaojiang fault. The Xianshuihe-Xiaojiang fault merged with the Red River fault at southern Yunnan. A series of Cenozoic north-south-trending half-graben basins were also developed along these faults, namely the Yuanmou Basin, Lufeng Basin, Dianchi Basin, Fuxian Basin, and Yiliang Basin (Fig. 1).

The N-S elongated Yuanmou Basin with an altitude of 1050 to 1400 m is bounded in its eastern side by the Yuanmou fault and a mountain consisting of the Jurassic Fengjiahe Formation and the Cretaceous Matoushan Formation, and in the western side by a range of the Precambrian Julin Group (Jiang et al., 1989). The late Neogene deposits were particularly well preserved in the southern part of the Yuanmou Basin with a thickness of ≥850 m. The beds tilt slightly eastward with a mean dip of ~9°. From bottom to top, the whole sedimentary sequence can be divided into four lithologic members: lacustrine and fluviolacustrine silty clay, silts and fine-grained sands (M1); fluvial and fluviolacustrine peaty clays, silts, silty clays and fine-grained sands (M2); fluvial silty clays interbedded with silts and fine-grained sands (M3); and fluvial and alluvial silty clays interbedded with sandy conglomerates (M4) (Pu and Qian, 1977; Qian and Zhou, 1991). The fluviolacustrine deposits also contain abundant Pleistocene mammalian, including hominin, fossils (Bien, 1940; Pei, 1961; Hu, 1973). Neither soil formation, which would indicate slowing or cessation of sedimentation, nor any significant depositional hiatus was observed in any part of the sequence in the field.

In this study, oriented paleomagnetic samples covering M4 to M1 were collected from the entire 260-m-thick Dapoqing (DPQ: 25.69°N, 101.92°E) section and the 644-m-thick Gantangmaoyi (GM: 25.65°N, 101.89°E) section. Block samples were orientated in situ using a magnetic compass. Differences between the 2000 China Geomagnetic Reference Field (CGRF) and the solar compass declination is less than 2°. Cubic samples with 2-cm edge length were cut in the laboratory for paleomagnetic measurements. The DPQ and GM sections (3 km apart) were correlated by using marker layers, a field traceable yellow sand layer and the highest peaty clay layer (HPCL). This field correlation was checked by sampling a ~60-m interval above and below the HPCL at GM where it overlaps the lower part of the DPQ section. Sampling intervals in both sections were 0.2–0.5 m, which provided a total of 1633 sampling levels.

3. Rock magnetic investigation

Anisotropy of magnetic susceptibility (AMS) was measured using a KLY-3s Kappabridge. The susceptibility tensor for each sample was calculated by a described method (Jelinek, 1978). To avoid potential problems associated with heating (Rochette et al., 1992), we completed the AMS measurements before any thermal demagnetization was conducted. In the 529 (DQP) and 1208 (GM) samples studied, most minimum susceptibility axes (K_{min}) are close to the vertical, perpendicular to the bedding plane, whereas the inclinations of the maximum axes (K_{max}) are very shallow (Fig. 2a). These results are typical for a normal sedimentary magnetic fabric that has been unperturbed since deposition.

Using the KLY-3s Kappabridge with a CS-3 high-temperature furnace, we performed magnetic susceptibility versus temperature (χ–T) analyses of the bulk sediment. Clear decreases in susceptibility at ~680ºC in most χ–T curves indicate that hematite is the main magnetic carrier with small amount of magnetite (T_c=585°C) in the studied samples (Fig. 2b). Stepwise isothermal remanent magnetization (IRM) acquisition behaviors show that samples have two magnetic components, one saturated at fields of 0.2–0.3 T but another unsaturated up to 1 T (Fig. 2c). The S-ratio (defined as $IRM_{0.3T}/IRM_{1T}$) is consistently low with a mean of 0.53±0.08 (N=543)

(Fig. 2d). Considering all the rock magnetic evidence together, we conclude that hematite is the dominant magnetic carrier in the Yuanmou Basin sediments. These observations question the consideration by Hyodo et al. (2002) that magnetite is the dominant magnetic carrier and AF demagnetization technique was applied to the major part of their collection.

4. Paleomagnetic analyses

In this study, total 1545 samples were subjected to progressive thermal demagnetization up to 680°C, with a 25–50°C interval below 585°C and a 10°C interval above, using a Magnetic Measurement Thermal Demagnetizer (MMTD Model 80). Remanence was measured using 2G cryogenic magnetometers (Models 755 and 760), which were installed in a magnetically shielded space (<300 nT). Representative demagnetization behaviors are presented in Fig. 3. A total of 88 peaty clay samples were subjected to a 150°C thermal demagnetization followed by AF demagnetization at peak fields up to 60 mT. Both methods were capable of isolating the characteristic remanent magnetization (ChRM) after removal of one or two soft secondary components of magnetization. The principal components direction was computed by a "least-squares fitting" technique (Kirschvink, 1980). Based on the rock magnetic analyses (i.e., hematite as the main remanence carrier), we determined the ChRM using high-temperature components (≥610°C) with at least four demagnetization steps trending towards the origin (Fig. 3). For AF demagnetized peaty clay samples we used a component ≥30 mT. Samples with maximum angular deviation larger than 15° were rejected for further analyses. Based on these criteria, 892 samples (~55%) had reliable ChRM directions. The virtual geomagnetic poles (VGPs) were determined from the ChRM vectors of those samples, and then their corresponding VGP latitudes were subsequently used to define the succession of magnetostratigraphic polarity (Fig. 4).

As mentioned above, Hyodo et al. (2002) have used the inadequate demagnetization technique to their collection. Moreover, they adopted ChRM directions of about 16% samples with a higher coercivity component from the center of a cluster instead of the principal component analysis method as the remanence carried by hematite can't be totally cleaned by AF demagnetization. Therefore, our new findings presented in this study supercede the previous ones.

As shown in Figure 4, nine reverse magnetozones (R1 to R9) and eight normal magnetozones (N1 to N8) are recognized in the DPQ and GM sections. Specifically, five magnetozones occur at DPQ: three with reverse polarity, R1 (0–113.5 m), R2 (164.85–218.85 m) and R3 (224.25–260.1 m); and two with normal polarity, N1 (113.5–164.85 m) and N2 (218.85–224.25 m). Below the HPCL marker layer at GM, there are six reverse magnetozones: R4 (258.1–272.55 m), R5 (332.8–353.95 m), R6 (387.05–443.8 m), R7 (459.05–481.4 m), R8 (507.4–606.7 m) and R9 (637.05–644.3 m); and six normal magnetozones: N3 (141.8–258.1 m), N4 (272.55–332.8 m), N5 (353.95–387.05 m), N6 (443.8–459.05 m), N7 (481.4–507.4 m) and N8 (606.7–637.05 m).

5. Discussion

5.1. Age constraints on the Yuanmou Basin sediments

Slight changes in bedding attitudes prevent this study from a meaningful local fold test. Instead, we calculated the mean ChRM directions and then performed the reversal test (McFadden and McElhinny, 1990) on sample levels. To do the test we rejected 186 samples with transitional directions (here designated polarity transition as having VGP latitudes less than 60°). The remaining 706 samples have a mean normal direction of D/I = 1.6°/27.1° (α_{95}=1.8°, N=254) and reversed direction of D/I = 181.3°/-28.2°) (α_{95}=1.4°, N=452); they positively pass the reversal test with A classification (McFadden and McElhinny, 1990). The overall mean direction is D/I = 1.4°/27.8° (α_{95}=1.1°), corresponding to the paleomagnetic pole at 79.1°N/266.7°E (A_{95}=2.8°). Thus, from this point of view we conclude that the observed paleomagnetic results are reliable. Although paleomagnetic results passed the reversal test, we noted an inclination shallowing of ~19° with respect to the synthetic European apparent polar wander path (APWP) of the same age proposed by Besse and Courtillot (2002). The low inclination may have been caused by syndepositional shallowing of the remanent inclination (Gilder et al., 2001). Several earlier studies revealed that inclination shallowing is a common phenomenon for sedimentary magnetism in Central Asia (e.g., Cogné et al., 1999; Gilder et al., 2001; Dupont-Nivet et al., 2002; Huang et al., 2004). The inclination shallowing seems to have equally affected both the normal and reversed directions for the Yuanmou data. Detailed discussion of the shallowing is beyond the scope of this paper.

Earlier studies have demonstrated that M4 is rich in mammalian fossils, known as the Yuanmou Fauna (Bien, 1940), which is similar taxonomically to the early Pleistocene Nihewan fauna in North China and the Villafranchian fauna in Europe (Bien, 1940; Hu, 1973; Pei, 1961; Qiu, 2000; Deng et al., 2008). By combining biochronological data and magnetostratigraphic results, the magnetozones determined for DPQ can readily be correlated to the geomagnetic polarity timescale (GPTS) (Berggren et al., 1995; Cande and Kent, 1995). DPQ magnetozones R1, R2 and R3 correspond to the Matuyama reverse chron; and N1 and N2, respectively to the Olduvai and Reunion normal subchrons of the GPTS (Fig. 4). GM magnetozones N3–N5 are correlated to the Gauss normal chron and its two reverse subchrons (the Kaena and the Mammoth), and magnetozones R6–R9, to the Gilbert reverse chron and its three normal subchrons (the Cochiti, the Nunivak and the Sidufjall). Therefore, by extrapolating the sedimentation rates of magnetozones N1–R2, we estimate the termination age of M4 to be ~1.37 Ma, instead of the Brunhes chron age estimated by Hyodo et al. (2002).

There was another major drawback of Hyodo et al.'s work besides incomplete removal of viscous remanence, they sampled only 78 sites for a 1300-m-thick section. Both the incomplete demagnetization and very coarse sampling can lead to missing or incorrect interpretation of polarities of this magnetostratigraphic sequence. In Hyodo et al.'s study there were only six paleomagnetic sampling sites in the Yuanmou Formation, corresponding to the M4 in this study; among them they claimed one normal magnetozone (represented by 14 samples of four sampling sites) with two reversal events (represented by 6 samples of two sampling sites). Their correlation of this normal magnetozone to the Brunhes chron is obviously incorrect. Magnetostratigraphic age of the Yuanmou hominin incisors will be detailed elsewhere (Zhu et al., 2008, manuscript submitted to Journal of Human Evolution).

On the basis of GPTS correlations of our densely sampled sequence, we estimate the base age of M1 to be ~4.9 Ma, which is significantly older than that of 3.6 Ma for the bottom of the Shagou Formation suggested by Hyodo et al. (2002). This suggests that the Yuanmou Basin subsided, possibly due to reactivation of the western branch of the Xianshuihe-Xiaojiang fault (Yuanmou fault), and started to accumulate sediments at the early Pliocene.

5.2. Sedimentary accumulation of the Yuanmou sequence

The built magnetochronology has provided an insight into the infilling process of the Yuanmou Basin. The variability in sedimentary accumulation of the Yuanmou Basin sequence is shown in Figure 5a. There exists high variability in sedimentation rates of the continental fluviolacustrine sequences in the Yuanmou Basin since ~4.9 Ma, which reveals four distinct stages during the infilling process of the basin. The first stage is from ~4.9 to 4.6 Ma, and has an accumulation rate of ~48 cm/kyr. The second, between 4.6 and 3.3 Ma, has a lower accumulation rate of ~12.5 cm/kyr. Nevertheless, we note that this accumulation rate is estimated based on only one point. The third stage, an interval of 3.2–3.1 Ma, has a very high accumulation rate of ~55 cm/kyr. And, the fourth stage from 3.1 to 1.4 Ma has an accumulation rate of ~26 cm/kyr. The variation of sedimentation rates can be attributed to either tectonics and/or environmental change. For example, during the early Pliocene (i.e., between 4.9 and 4.6 Ma), the development of the Yuanmou paleolake was initiated due to fault-controlled subsidence, and sediments rich in conglomerates were accumulated. The high sedimentation rate during this stage was associated with the initial formation of the basin and was very likely due to rapid tectonic subsidence. The lower sedimentation rate during 4.6–3.3 Ma was probably mainly related to climate change, when tectonics imparted weak control on basin infilling and numerous peaty clay layers were deposited under warm and wet conditions. The substantially higher sedimentation rate during 3.2–3.1 Ma is also probably indicative of an episode of rapid tectonic subsidence, which was followed by a significant decrease in sedimentation rate during 3.1−1.4 Ma, when a distinctive sequence of floodplain silty clay and silts was developed.

5.3. Possible vertical-axis tectonic rotation

According to modern observations on the deformation in Tibet and its surrounding areas, England and Molnar (1990) proposed that the crustal blocks between the east-striking faults in the eastern part of the Tibetan Plateau rotated clockwise at 1–2°/myr. Based on the sedimentological study, Wang and Burchfiel (2000) proposed that crust in the southeastern part of the Tibetan Plateau has internally deformed and clockwisely rotated. Importantly, our new paleomagnetic data provide an opportunity to discuss the timing of possible vertical-axis rotations, which were lacking in most previous paleomagnetic studies. To this end, we calculated the mean directions of each of the seventeen polarity units (excluding samples with transitional directions). Results are shown in Table 1 and Figure 5b. These declination means may be paleomagnetically combined into three distinct groups (I to III) with overlaps between neighbor groups if the errors are taken into consideration. Specifically, the Fisher mean declinations of Group I (polarities R1 to R3, 2.58−1.37 Ma), Group II (polarities N3 to N6, 4.29–2.58 Ma) and Group III (polarities R7 to R9, 4.91–4.29 Ma) are -2.8°±1.6°, 2.0°±1.8° and 9.2°±2.1°, respectively, strongly suggesting a progressive vertical-axis clockwise rotation of about 12° from 1.4 Ma to 4.9 Ma for the Yuanmou Basin. Because of the sufficient time intervals used (> 600 kyr), the paleosecular variation influence on these mean directions should be averaged out. Considering the number of samples used in statistics (N=174 to 338), the measurement error potentially related to the imprecision of sampling orientation most likely had an insignificant effect. Moreover, the slight tilting of beds has been corrected and the field observation of the sampled sections does not show any significant internal deformation, such as faulting. Therefore, we tend to interpret these grouped means of declinations to be the resultant of progressive vertical-axis clockwise tectonic rotations of the studied basin.

Understanding of these progressive vertical-axis tectonic rotations may enhance the debate on the consequence of the India-Eurasia collision. Because of lack of paleomagnetic data of the same timing resolution from the neighbor blocks, we discuss them in the geographic (absolute) frame and compare them with stable Europe reference (Besse and Courtillot, 2002). Groups I and II show slight differences of -2.8°±1.6° and 2.0°±1.8° at the 95% confidence level with respect to the geographic pole, respectively. If the 2σ statistic probability is taken into account, these differences become insignificant. However, Group III presents significant difference of mean declination in clockwise with geographic north at 95% confidence level. That may interpret that the Yuanmou Basin has experienced a progressive clockwise rotation in the geographic (absolute) frame. If compared to the expected declination calculated from the synthetic European APWP of 3 Ma (λ_p=86.3°N, φ_p=172.0°E, A_{95}=2.6°; Table 1) proposed by Besse and Courtillot (2002), we note that Group I apparently rotated -6.7°±2.8° counterclockwise, Group II -1.9°±2.8° in the same sense, however, and Group III rotated 5.3°±3.0° clockwise (Table 1). In other words, an earlier clockwise rotation of the Yuanmou Basin was followed by a later counterclockwise rotation relative to the expected direction determined from reference European APWP. An accumulated relative rotation of about 12° occurred, therefore, for the studied section from 1.4 to 4.9 Ma, which indicates an apparent rapid relative rotation of about 4°/myr. Of course, we have noticed that this comparison and its consequent tectonic interpretation may be obscured due to the following reasons: 1) Several active tectonic structures are located from stable Europe and the studied area, such as Altay, Tianshan, Altyn Tagh; 2) The process of India-Eurasia collision presents a continuous nature in the time scale of this study (Patriat and Achache, 1984), and no obvious tectonic evidence to rotate the Yuanmou Basin in different senses from such a short interval from 4.9 to 1.4 Ma.

The clockwise rotation of the Yuanmou Basin obtained from this study is coherent with field observations and GPS measurement carried out around the eastern Himalayan syntaxis (England and Molnar, 1990; Leloup et al., 1995; Wang et al., 1998; Tapponnier et al., 2001). This rotation could be interpreted as evidence for the transformation of the Red River fault from left-lateral to right-lateral (e.g., Leloup et al. 1995). In brief, the regional clockwise rotation of the Yuanmou Basin could be linked to the displacement on the Xianshuihe-Xiaojiang left-lateral strike-slip fault and motion associated with the Red River fault.

6. Conclusions

This paleomagnetic study has shown that the Yuanmou Basin near the southeastern margin of the Tibetan Plateau began to accumulate sediments in the early Pliocene. Seventeen polarity units (9 reverse and 8 normal) were determined for the 850-m thick sequence, the corresponding age spanned from 4.9 to 1.4 Ma. The sedimentation rate varied from 12.5 to 55 cm/kyr, possibly related to tectonics and/or climate changes. Importantly, the observed discordant declinations suggest significant clockwise vertical-axis tectonic rotations of the Yuanmou Basin since the early Pliocene time, which provides constraints on activities of major fault systems in the adjacent region during the past ~4.9 Ma. In summary, the magnetochronology of the Yuanmou sequence chronicles the late Neogene infilling process in the Yuanmou Basin and tectonic rotations in the southeastern Tibetan Plateau.

Acknowledgements

Financial assistance was provided by the NSFC grant 40221402 and CAS. RP acknowledges support by the U.S. National Science Foundation (BCS 0218511) and the Smithsonian's Human Origins Program. Drs. K.A. Hoffman, G. Dupont-Nivet, Y. Chen and an anonymous reviewer are highly appreciated for their very constructive comments on an earlier manuscript. Craig Jones provided paleomagnetic software. We thank Drs. J. L. Xiao and Z. G. Chang for field assistance.

References

An, Z.S., Kultzbach, J.E., Prell, M.L., Porter, S.C., 2001. Evolution of the Asian monsoons and phased uplift of the Himalayan-Tibetan plateau since late Miocene times. Nature 411, 62–66.

An, Z.S., Wang, S.M., Wu, X.H., Chen, M.Y., Sun, D.H., 1999. Eolian evidence from the Chinese Loess Plateau: the onset of the Late Cenozoic Great Glaciation in the northern Hemisphere and Qinghai-Xizang Plateau uplift forcing. Sci. China (Ser. D) 32, 258–271.

Avouac, J.P., Tapponnier, P., 1993. Kinematic model of active deformation in central Asia. Geophys. Res. Lett. 20, 895–898.

Berggren, W.A., Kent, D.V., Swisher III, C.C., Aubry, M.-P., 1995. A revised Cenozoic geochronology and chronostratigraphy in time scales and global stratigraphic correlations: A unified temporal framework for an historical geology, in: Berggren, W.A., Kent, D.V., Aubry, M.-P., Hardenbol, J. (Eds.), Geochronology, Timescales, and Stratigraphic Correlation, Spec. Publ. No. 54, Society of Economic Paleontologists and Mineralogists, Tulsa, OK, pp. 129–212.

Besse, J., Courtillot, V., 2002. Apparent and true polar wander and the geometry of the geomagnetic field over the last 200 Myr. J. Geophys. Res. 107, 2300, doi:10.1029/2000JB000050.

Bien, M.N., 1940. Preliminary observation on the Cenozoic geology of Yunnan. Bull. Geol. Soc. China 20, 179–194.

Butler, R.F., 1992. Paleomagnetism: Magnetic Domains to Geologic Terranes. Blackwell Scientific Publications, Boston.

Cande, S.C., Kent, D.V., 1995. Revised calibration of the geomagnetic polarity timescale for the Late Cretaceous and Cenozoic. J. Geophys. Res. 100, 6093–6096.

Chen, Y., Gilder, S., Halim, N, Cogné, J.P., Courtillot, V., 2002. New paleomagnetic constraints on central Asian kinematics: Displacement along the Altyn Tagh fault and rotation of the Qaidam Basin. Tectonics 21, 1042, doi:10.1029/2001TC901030.

Chung, S.L., Lo, Q.H., Lee, T.Y., Zhang, Y.Q., Xie, Y.W., Li, X.H., Wang, K.L., Wang, P.L., 1998. Diachronous uplift of the Tibetan plateau starting 40 Myr ago. Nature 394, 769–773.

Clark, M.K., House, M.A., Royden, L.H., Whipple, K.X., Burchfiel, B.C., Zhang, X., Tang, W., 2005. Late Cenozoic uplift of southeastern Tibet. Geology 33,

ACCEPTED MANUSCRIPT

525–528.

Cogné, J.P., Halim, N., Chen, Y., Courtillot, V., 1999. Resolving the problem of shallow magnetizations of Tertiary age in Asia: Insights from paleomagnetic data from the Qiangtang, Kunlun, and Qaidam blocks (Tibet, China), and a new hypothesis. J. Geophys. Res. 104, 17715–17734, doi: 10.1029/1999JB900153.

Deng, C.L., Zhu, R.X., Zhang, R., Ao, H., Pan, Y.X., 2008. Timing of the Nihewan formation and faunas. Quat. Res. 69, 77–90.

Dupont-Nivet, G., Bulter, R.F., Yin, A., Chen, X., 2002. Paleomagnetism indicates no Neogene rotation of the Qaidam Basin in North Tibet during Indo-Asian collision. Geology 30, 263–266.

Dupont-Nivet, G., Bulter, R.F., Yin, A., Chen, X., 2003. Paleomagnetism indicates no Neogene rotation of the Northeastern Tibetan plateau. J. Geophys. Res. 108(B8), 2386, doi: 10.1029/2003JB002399.

Dupont-Nivet, G., Horton, B.K., Zhou, J., Waanders, G.L., Butler, R.F., Wang, J., 2004. Paleogene clockwise tectonic rotation of the Xining-Lanzhou region, northeastern Tibetan Plateau. J. Geophys. Res. 109, B04401, doi: 10.1029/2003JB002620.

England, P., Molnar, P., 1990. Right-lateral shear and rotation as the explanation for strike-slip faulting in eastern Tibet. Nature 344, 140–142.

England, P.C., Houseman, G.A., 1988. The mechanics of the Tibetan Plateau. Philos. Trans. R. Soc. London 326, 301–320.

Gilder, S., Coe, R.S., Wu, H.R., Kuang, G.D., Zhao, X.X., Wu, Q., Tang, X.Z., 1993. Cretaceous and Tertiary paleomagnetic results from southeast China and their tectonic implications. Earth Planet. Sci. Lett. 117, 637–652.

Gilder, S., Chen, Y., Sen, S., 2001. Oligo-Miocene magnetostratigraphy and rock magnetism of the Xishuigou section, Subei (Gansu Province, western China) and implications for shallow inclinations in central Asia. J. Geophys. Res. 106, 30505–30522, doi: 10.1029/2001JB000325.

Guo, Z.T., Ruddiman, W.F., Hao, Q.Z., Wu, H.B., Qiao, Y.S., Zhu, R.X., Peng, S.Z., Wei, J.J., Yuan, B.Y., Liu, T.S., 2002. Onset of Asian desertification by 22 Myr ago inferred from loess deposits in China. Nature 416, 159–163.

Hu, C.Z., 1973. Ape-man teeth from Yuanmou, Yunnan. Acta Geologica Sinica (1), 65–72.

Huang, K., Opdyke, N.D., Li, J., Peng, X., 1992. Paleomagnetism of Cretaceous rocks from eastern Qiangtang terrane of Tibet. J. Geophys. Res. 97, 1789–1799.

Huang, B.C., Wang, Y.C., Liu, T., Yang, T.S., Li, Y.A., Sun, D.J., Zhu, R.X., 2004. Paleomagnetism of Miocene sediments from the Turfan Basin, Northwest China: no significant vertical-axis rotation during Neotectonic compression within the Tian Shan Range, Central Asia. Tectonophysics 384, 1–21.

Hyodo, M., Nakaya, H., Urabe, A., Saegusa, H., Xue, S., Yin, J., Ji, X., 2002. Paleomagnetic dates of hominid remains from Yuanmou, China, and other Asian sites. J. Hum. Evol. 43, 27–41.

Jelinek, V., 1978. Statistical processing of anisotropy of magnetic susceptibility measured on groups of specimens. Stud. Geophys. Geod. 22, 50–62.

Jiang, N.R., Sun, R., Liang, Q.Z., 1989. The Late Cenozoic Stratigraphy and Paleotology in Yuanmou Basin, Yunnan, China. Yunnan Science Press, Kunming.

King, R.W., Shen, F., Clark, Burchfiel, B.C., Royden, L.H., Wang, E., Chen, Z., Liu, Y., Zhang, X.-Y., Zhao, J.-X., Li, Y., 1997. Geodetic measurement of crustal motion in southwest China. Geology 25, 179–182.

Kirschvink, J.L., 1980. The least-squares line and plane and the analysis of palaeomagnetic data. Geophys. J. R. Astron. Soc. 62, 699–718.

Leloup, P.H., Lacassin, V, Tapponnier, P., Schärer, U., Zhong, D.L., Liu, X.H., Zhang, L.S., Ji, S.C., Trinh, P.T., 1995. The Ailao Shan-Red River shear zone (Yunnan, China), Tertiary transform boundary of Indochina. Tectonophysics 251, 3–84.

Li, P., Qian, F., Ma, X., Pu, Q., Xing, L., Ju, S., 1976. Preliminary study on the age of the Yuanmou Man by paleomagnetic technique. Sci. China (6), 579–591 (in Chinese).

McFadden, P.L., McElhinny, M.W., 1990. Classification of the reversal test in palaeomagnetism. Geophys. J. Int. 103, 725–729.

Otofuji, Y., Inoue, S., Funahara, S., Murata, F., Zheng, X., 1990. Palaeomagnetic study of eastern Tibet- deformation of the Three Rivers region. Geophys. J. Int. 103, 85–94.

Patriat, P., Achache, J., 1984. India–Eurasia collision chronology has implications for crustal shortening and driving mechanisms of plates. Nature 311, 615–621.

Pei, W.C., 1961. Fossil Mammals of early Pleistocene age from Yuanmo (Ma-kai) of Yunnan. Vertebrata Palasiatica 3(1), 16–31.

Peltzer, G., Tapponnier, P., 1988. Formation and evolution of strike-slip faults, rifts, and basins during the India-Asia collision: an experimental approach. J. Geophys. Res. 93, 15085–15117.

Pu, Q.Y., Qian, F., 1977. Study on the fossil human strata—the Yuanmo Formation. Acta Geologica Sinica (1), 89–100.

Qian, F., Pu, Q.Y., Wang, D.S., 1984. The discovery of the teeth of Yuanmou Man, in: Zhou, G.X., Zhang, X.Y. (Eds.), Yuanmou Man. Yunnan People's Press, Kunming, pp. 3–7.

Qian, F., Zhou, G.X., 1991. Quaternary Geology and Paleoanthropology of Yuanmou, Yunnan, China. Science Press, Beijing.

Qiu, Z.X., 2000. Nihewan fauna and Q/N boundary in China. Quat. Sci. 20, 142–154.

Rea, D.K., Snoeckx, H., Joseph, L.H., 1998. Late Cenozoic eolian deposition in the North Pacific: Asian drying, Tibetan uplift, and cooling of the northern hemisphere. Paleoceanography 13, 215–224.

Rochette, P., Jackson, M., Aubourg, C., 1992. Rock magnetism and the interpretation of anisotropy of magnetic susceptibility. Rev. Geophys. 30, 209–226.

Sato, K., Liu, Y.Y., Wang, Y.B., Yokoyama, M., Yoshioka, S., Yang, Z.Y., Otofuji, Y., 2007. Paleomagnetic study of Cretaceous rocks from Pu'er, western Yunnan, China: Evidence of internal deformation of the Indochina block. Earth Planet. Sci. Lett. 258, 1–15.

Tapponnier, P. Xu, Z.Q., Roger, F., Meyer, B., Arnaud, N., Wittlinger, G., Yang, J.S., 2001. Oblique stepwise rise and growth of the Tibet Plateau. Science 294, 1671–1677.

Wang, E., Burchfiel, B.C., Royden, L.H., Chen, L., Chen, J., Li, W., 1998. The late Cenozoic Xianshuihe–Xiaojiang, Red River, and Dali fault systems of southwestern Sichuan and Central Yunnan, China. Geological Society of America Special Paper 327, 108.

Wang, E., Burchfiel, B.C., 2000. Late Cenozoic to Holocene deformation in southwestern Sichuan and adjacent Yunnan, China, and its role in formation of the southeastern part of the Tibetan Plateau. Geol. Soc. Am. Bull. 112, 413–423.

Wu, X., Poirier, F.E., 1995. Human Evolution in China: A Metric Description of the Fossils and a Review of the Sites. Oxford University Press, New York.

Yin, A., Harrison, T.M., 2000. Geologic evolution of the Himalayan-Tibetan orogen. Annu. Rev. Earth Planet. Sci. 28, 211–80.

Zhang, W.Y., et al., 1983. The Marine and Continental Tectonic Map of China and its Environs (Scale 1:5,000,000). Science Press, Beijing.

Zhu, Z.W., Hao, T., Zhao, H., 1988. Paleomagnetic study on the tectonic motion of Pan-Xi block and adjacent area during Yin Zhi - Yanshan period. Acta Geophysica Sinica 31, 420–431.

Zhu, R.X., Potts, R., Pan, Y.X., Yao, H.T., Lü, L.Q., Zhao, X., Gao, X., Cheng, L.W., Deng, C.L., 2008. Evidence of earliest *Homo erectus* in East Asia. Submitted to J. Hum. Evol.

FIGURE CAPTIONS

Fig. 1. Sketch tectonic map (a) and detailed geological map (b) showing sedimentary basins (the numbers 1–5 in (a)) and major fault systems in the eastern Tibetan Plateau and Yunnan. 1, Yuanmou Basin; 2, Lufeng Basin; 3, Dianchi Lake; 4, Fuxian Lake; 5, Yiliang Basin. The filled square in (a) is the location of a Global Positioning System station named DLH shown in King et al. (1997).

Fig. 2. Rock magnetic results. (a) Anisotropy of magnetic susceptibility (AMS) diagram. Squares (circles) stand for K_{max} (K_{min}). (b) Representative χ–T curves (heating curves only). (c) Representative normalized IRM acquisition curves. (d) Variation of the S ratio ($IRM_{0.3T}/IRM_{1T}$) with depth (upper 647 m, correlation between two sections, see text).

Fig. 3. Representative orthogonal plots of the Dapoqing, DPQ (a–d) and Gantangmaoyi, GM (e–l) sections. All directions are tilt-corrected. Open (solid) circles are plotted on vertical (horizontal) plane. Thermal treatment levels are marked in degree Celsius. See Figure 4 for depths of the samples.

Fig. 4. Lithostratigraphy and magnetic polarity stratigraphy at Dapoqing, DPQ (a–c) and Gantangmaoyi, GM (e–g) and their correlation with the geomagnetic polarity timescale, GPTS (d) (Cande and Kent, 1995; Berggren et al., 1995). The highest peaty

clay maker layer (HPCL) and the lithologic member (M) boundaries are shown. VGP Lat, latitude of virtual geomagnetic pole; R, reverse polarity; and N, normal polarity. The stars show the GPS points.

Fig. 5. (a) Magnetic polarities identified in the DPQ and GM sections of the Yuanmou Basin. (b) Variation of the sedimentation rates of polarity units as a function of ages. The empty and solid circles represent data of the DPQ and GM sections, respectively. The solid line shows the averaged sedimentation rates of the four stages during the infilling process of the Yuanmou Basin. (c) Variation of the Fisher mean declinations of polarity units as a function of ages. The diamonds show data of the DPQ section; the squares, of the combined DPQ and GM sections; and the triangles, of the GM section. Numbers next to the symbols are sample numbers of the polarity unit that were used for the calculation of the mean. The vertical bars represent the age intervals. The horizontal error bars are the 95% confidence limit of the declinations. These declination means can be paleomagnetically combined into three distinct groups (I, II and III). The dashed line shows the expected declination from the referenced European paleomagnetic pole of 3 Myr.

Table 1. Paleomagnetic poles from this study together with expected declination and rotations[a]

phases	Depth (m)	Age (Ma)	N	D_s (°)	I_s (°)	α_{95} (°)	λ_p (°N)	φ_p (°E)	A_{95} (°)	$D_{exp} \pm \Delta D_{exp}$ (°) Europe	$R \pm \Delta R$ (°) Europe
I	0-141.8	1.37–2.58	5	-2.8	26.3	1.6	77.3	297.3	2.6		-6.7±2.8
II	141.9-459.1	2.58–4.29	7	2.0	25.6	1.8	77.3	270.0	1.3	3.9±2.9	-1.9±2.8
III	459.2-644.3	4.29–4.91	5	9.2	32.8	2.1	78.7	225.2	3.5		5.3±3.0
I, II, III	0-644.3	1.37–4.91	17	1.4	27.8	1.1	79.1	266.7	2.8		-2.5±2.5

[a] N, the numbers of polarities. D_s, I_s and α_{95} are mean declination, inclination and 95% confidence limit, respectively. λ_p and φ_p are latitude and longitude of paleomagnetic pole from this study, respectively. A_{95} is the radius of 95% confidence region of paleomagnetic poles. D_{exp} and ΔD_{exp} are the expected declination and its confidence limit at the coeval referenced pole, respectively. The referenced European paleomagnetic pole of 3 Myr is at λ_p=86.3°N, φ_p =172.0°E (A_{95}=2.6°) (data from Besse and Courtillot, 2002). The vertical-axis rotation with 95% confidence limit, $R \pm \Delta R$, were calculated after Butler (1992).

Fig. 1

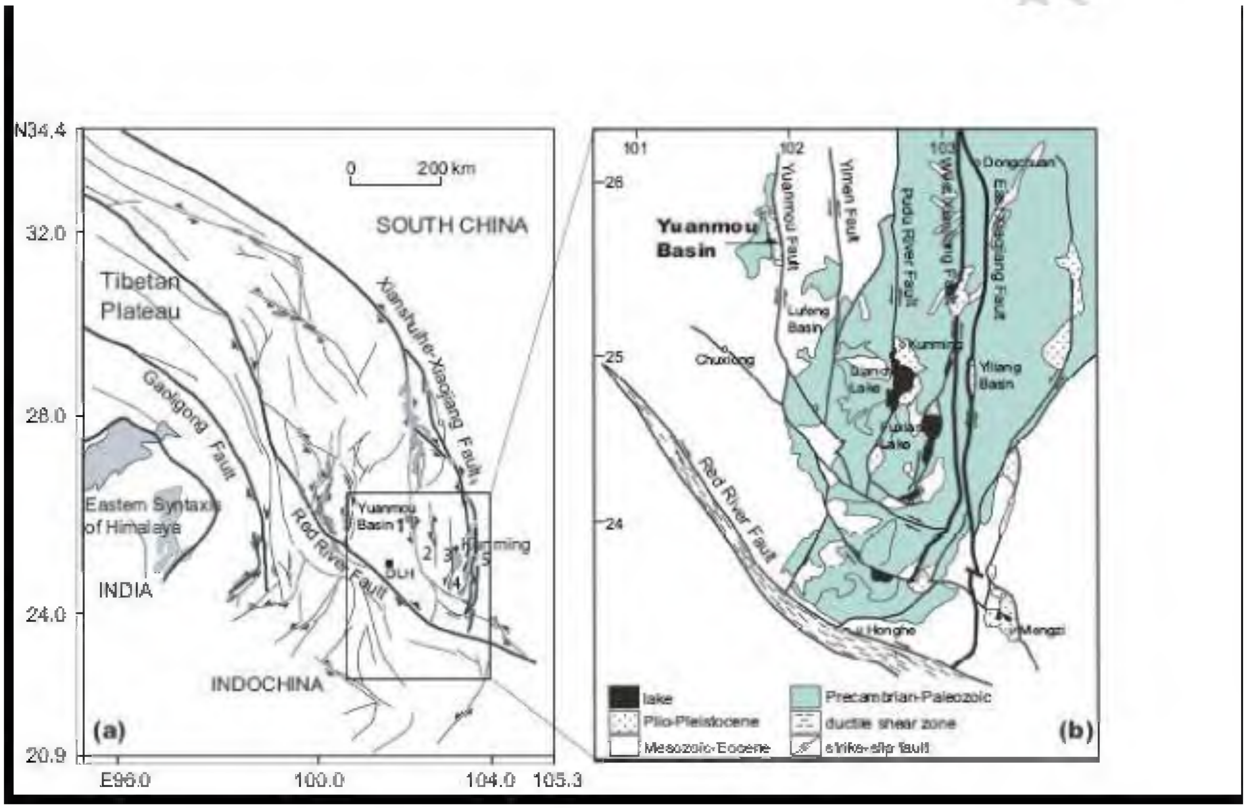

N34.4
32.0
28.0
24.0
20.9
E96.0
100.0
104.0
105.3
0
200 km
SOUTH CHINA
Tibetan Plateau
Xianshuihe-Xiaojiang Fault
Gaoligong Fault
Eastern Syntaxis of Himalaya
INDIA
Red River Fault
Yuanmou Basin
Kunming
INDOCHINA
(a)
101
102
103
26
25
24
Yuanmou Basin
Yuanmou Fault
Yimen Fault
Pudu River Fault
West Xiaojiang Fault
East Xiaojiang Fault
Dongchuan
Lufeng Basin
Chuxiong
Kunming
Yiliang Basin
Dianchi Lake
Fuxian Lake
Red River Fault
Honghe
Mengzi
lake
Plio-Pleistocene
Mesozoic-Eocene
Precambrian-Paleozoic
ductile shear zone
strike-slip fault
(b)

Fig. 2

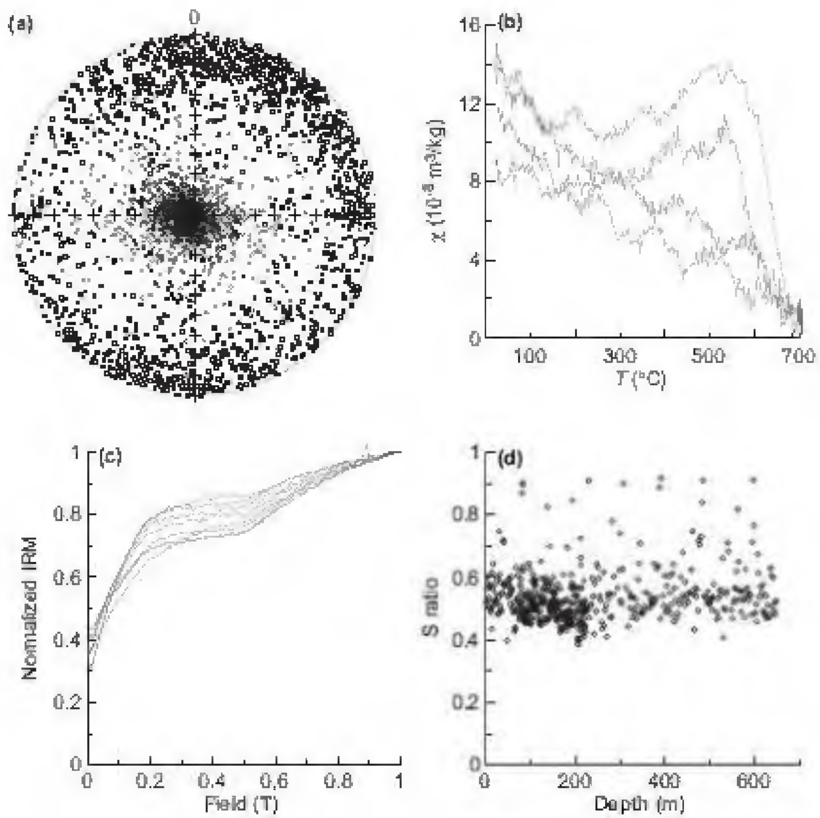

552 Fig. 3

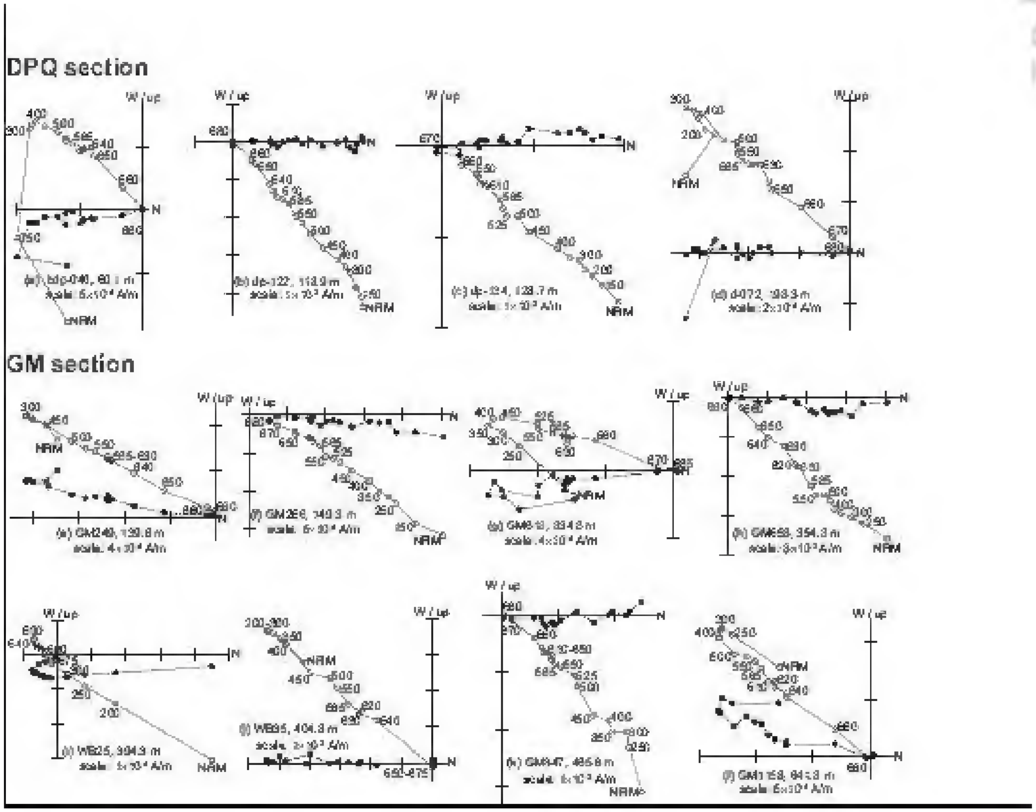

553

Fig. 4

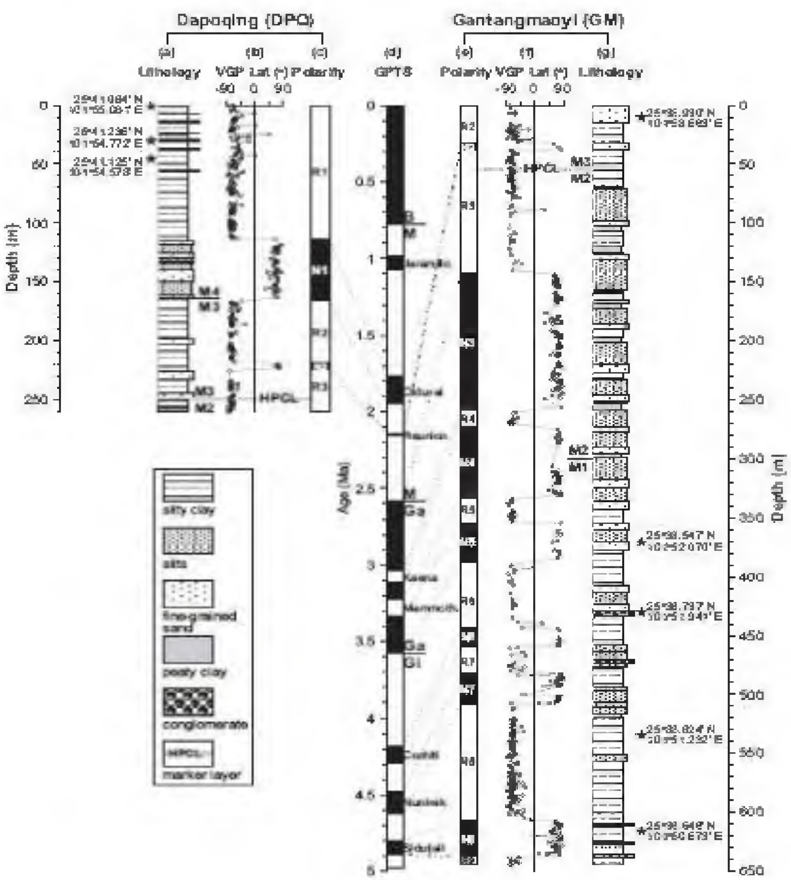

Dapoqing (DPQ)
Gantangmaoyi (GM)
(a) Lithology
(b) VGP Lat (°)
(c) Polarity
(d) GPTS
(e) Polarity
(f) VGP Lat (°)
(g) Lithology
Depth (m)
Age (Ma)
HPCL
silty clay
silts
fine-grained sand
peaty clay
conglomerate
marker layer

Fig. 5

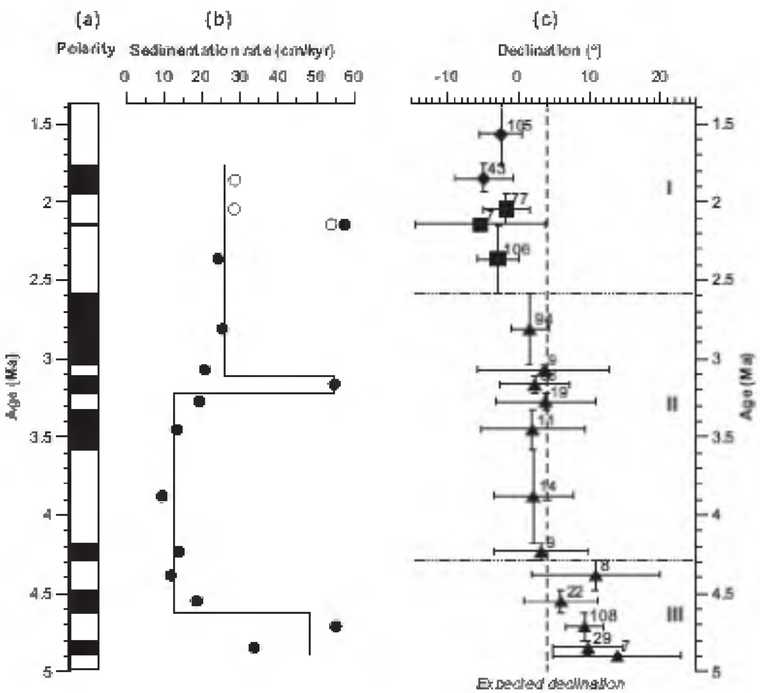

(a)
Polarity
(b)
Sedimentation rate (cm/kyr)
(c)
Declination (°)
Age (Ma)
I
II
III
Expected declination